

Chapter 6

One-Dimensional Propagation in Liquids

It is well known that the additional degrees of freedom of constituent molecules in a liquid compared to molecules in a solid lead to more complicated interactions between the liquid and an electromagnetic field. Propagation of an intense beam through a liquid can result not only in the instantaneous optical Kerr effect, but in molecular reorientation, molecular redistribution, and Raman excitations of rotation and libration as well [124, 152]. Molecular reorientation is a rotation of a molecule to reduce the energy of the system in response to a field induced dipole moment of that molecule. Molecular reorientation typically occurs on a timescale of 10^{-11} s [124]. Molecular redistribution is also a response of the material to a field induced dipole moment and involves the local rearrangement of molecules in the field to minimize the energy of induced dipole-induced dipole interactions between molecules. This rearrangement has a response time in the sub-picosecond range [124]. The response times for rotation and libration are typically on the order of 100 fs. Electrostriction, which is an increase in the density of a material due to the presence of an applied field, typically has a response time of approximately 100 ns in liquids [124]. Most all of these processes involve a response time that is longer than the duration of our 80-100 fs pulses. Rotation and libration respond on a timescale that is very close to the duration of our pulses. Because of these long response times, none of these processes should lead to an observable effect in our experiments. We expect, therefore, to observe the same processes involved

in propagation of short pulses in liquids as were observed in propagation through fused silica in one dimension, namely the electronic Kerr effect and group velocity dispersion.

Interestingly, however, Nibbering *et al.* have reported a non-instantaneous non-linear response in methanol with a response time of 27 fs [94]. Their experiment involves propagation of 804 nm, 24 mJ, 150 fs pulses through a known reference material and an unknown sample. The spectrum before and after each propagation is measured. Spectral changes upon propagation through the reference material yield the initial pulse intensity. The initial pulse intensity is then used with the second spectral measurement to determine the nonlinear index of refraction of the unknown sample. Nibbering asserts that this measurement is evidence that the optical Kerr effect in methanol is dominated by a nuclear rather than a purely electronic term. Their work assumes that the non-instantaneous response can be modeled by a single-sided exponential:

$$n(t) = \int_{-\infty}^t \frac{n_2 I(t')}{\tau} \exp\left(-\frac{t-t'}{\tau}\right) dt'. \quad (6.1)$$

This chapter investigates the propagation of $\sim 80 - 120$ fs pulses in two liquids: methanol and water. Methanol is studied with the purpose of repeating Nibbering's measurement using a different technique and thereby confirming or disproving the reported non-instantaneous nonlinearity. Water is investigated for two reasons. Propagation issues involved in sending short pulses through water, particularly the nonlinear index of refraction of liquid water, is of considerable interest in the biological sciences. Short pulse lasers are finding application in research involving the human body, especially with regard to surgical techniques [153, 154, 155]. In addition, water is studied because it is a hydrogen-bonded, polar liquid composed of relatively small molecules and, as such, is suitable for testing for systematic errors in the measurement. To wit, if both liquids show the same non-instantaneous response, the integrity of the measurement technique can be questioned. If the experiments in water reveal a purely instantaneous response, however, while the experiments in methanol do not, then it is

likely that the non-instantaneous nonlinearity is real and not merely an artifact of the measurement technique.

6.1 Methanol Studies

6.1.1 Stationary Cell Measurements

Experiment

Pulses from the compressor stage of the laser system described in Chapter 3 propagate unfocused to the sample. The unfocused beam propagates approximately as a plane wave in the sample, with a diameter of 5 mm (FWHM). The energy per pulse of 227 μJ corresponds to a peak power of 2.6 GW. Because of the high energy of the pulses, the beam is not spatially filtered. Plane-wave propagation within the sample is verified explicitly by measuring the beam size before and after propagation through the sample. To within the experimental error due to the pixel size of the CCD camera, the beam size is unchanged. The spectroscopic grade methanol sample is placed in a 1 cm path length Starna spectrophotometer cuvette. Propagation through only the two 1-mm-thick cell walls of the empty cuvette is found to have negligible effect on the pulse at this intensity.

An interesting problem arises in attempting to perform FROG measurements with this experimental set up. When methanol is added to the cuvette, the beam acquires a dynamic spatial modulation after propagation. If one observes the liquid sample with a flashlight in a dark room, one can see a convective-type current in the liquid and small dust-sized particles moving in a circular pattern. Repeated cleaning of the cuvette makes no difference in this behavior. If the sample is allowed to sit undisturbed for ~ 24 hours, however, the liquid becomes calm, and the beam passes through with no observable spatial modulation. All data presented in this chapter were acquired after

a minimum 24 hour wait period.

Data

Figure 6.1 shows the measured intensity and phase of a pulse prior to and after propagation through the methanol sample. The input field is shown in (a) and the field after propagation is shown in (b). In both graphs, the solid line represents the intensity, and the points represent the phase. The upward curvature of the phase in (a) is evidence of an initially slightly downchirped input. After propagation through the methanol, the pulse is noticeably upchirped as a result of the positive group velocity dispersion and the positive nonlinear index of refraction n_2 . In addition, the peak of the phase curvature has been shifted slightly toward the trailing edge of the pulse.

Model and Results

Since conditions have been chosen such that the pulse propagates through the sample as a plane wave, the propagation can be modeled using a (1+1)-dimensional nonlinear Schrödinger equation:

$$\frac{\partial \mathcal{E}}{\partial z} + i \frac{k''}{2} \frac{\partial^2 \mathcal{E}}{\partial t^2} - i \frac{2\pi n_2}{\lambda} |\mathcal{E}|^2 \mathcal{E} = 0. \quad (6.2)$$

The second term of this equation accounts for group velocity dispersion, and the third term gives the instantaneous nonlinearity. The measured input field shown in Fig. 6.1(a) is used as an initial condition of this model, with $k'' = 290 \text{ fs}^2/\text{cm}$ [156] and $n_2 = 4 \times 10^{-16} \text{ cm}^2/\text{W}$. The propagated field is then calculated using a split-step technique [107, 129] and is shown in Fig. 6.2(a) along with the measured field for comparison. The calculated intensity and phase are given by the dashed line and the crosses, respectively. The simulation was performed using a range of different n_2 values around those found in the literature [94, 157], and no significant difference in the fit was observed. As illustrated by this example, the simple model, including reasonable values for the material parameters and an instantaneous response time for the nonlinearity,

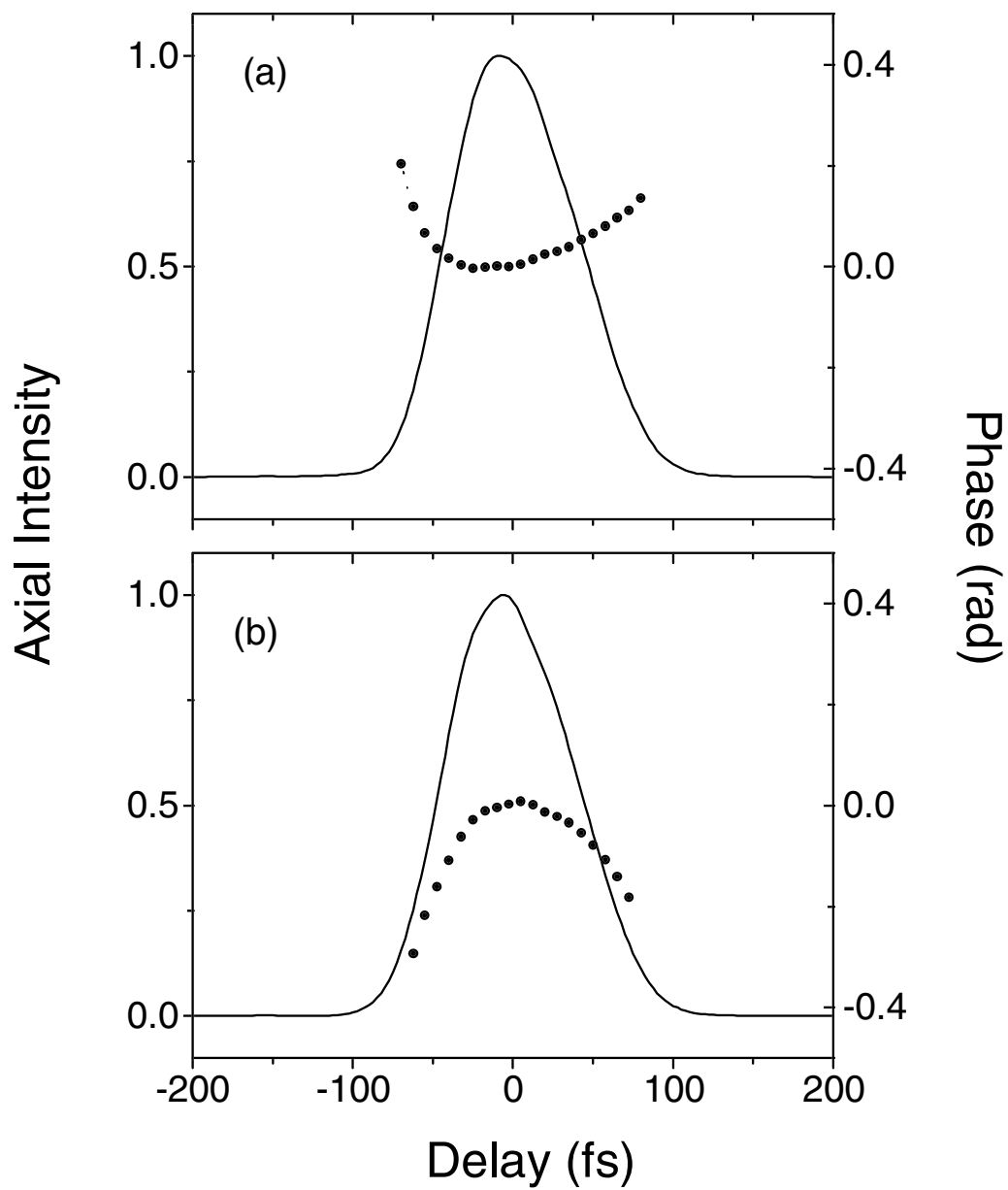


Figure 6.1: Intensity (solid lines) and phase (points) of a pulse both (a) prior to and (b) after propagation through a 1-cm sample of methanol.

fails to match the experimentally measured phase, especially the shift in the phase to later times.

This shortcoming in the model can be corrected by phenomenologically including a non-instantaneous response of the nonlinearity such that the term

$$n_2|\mathcal{E}|^2$$

in Eq. (2) is replaced by [114]

$$\int_{-\infty}^t \frac{n_2|\mathcal{E}(t')|^2}{\tau} \exp\left(-\frac{t-t'}{\tau}\right) dt' \quad (6.3)$$

where τ is the exponential response time of the nonlinearity. Equation 6.3 is the same representation of the non-instantaneous nonlinearity used by Nibbering *et al* [94].

Figure 6.2(b) shows the results of the model including the non-instantaneous response term of Eq. 6.3 with $\tau = 10$ fs. The measured input field of Fig. 6.1(a) was again used as an initial condition of the model. Inclusion of the non-instantaneous response correctly predicts the observed shifting of the peak of the phase toward the trailing edge of the pulse. The calculated phase best matches the experimentally determined phase when values of $n_2 = 4 \times 10^{-16}$ cm²/W and $\tau = 10$ fs are used.

An interesting feature of the data in Fig. 6.2 is the extremely small value of the exponential response time τ . As mentioned previously, response times for electrostriction, molecular reorientation, molecular redistribution, and molecular librations are all too slow to explain the observed non-instantaneous nonlinearity. As seen in the one-dimensional experiments with fused silica presented in Chapter 4, vibrational Raman does not come into play unless much higher intensities (and therefore larger pulse bandwidths due to self-phase modulation) are used. Thermal effects occur on very long timescales relative to the length of our pulses. Because a single FROG measurement requires approximately five minutes to acquire and the repetition rate of the laser is 1 kHz, it is possible that thermal effects could appear in these stationary cell measurements. Nibbering's work does not mention the sample conditions. To determine

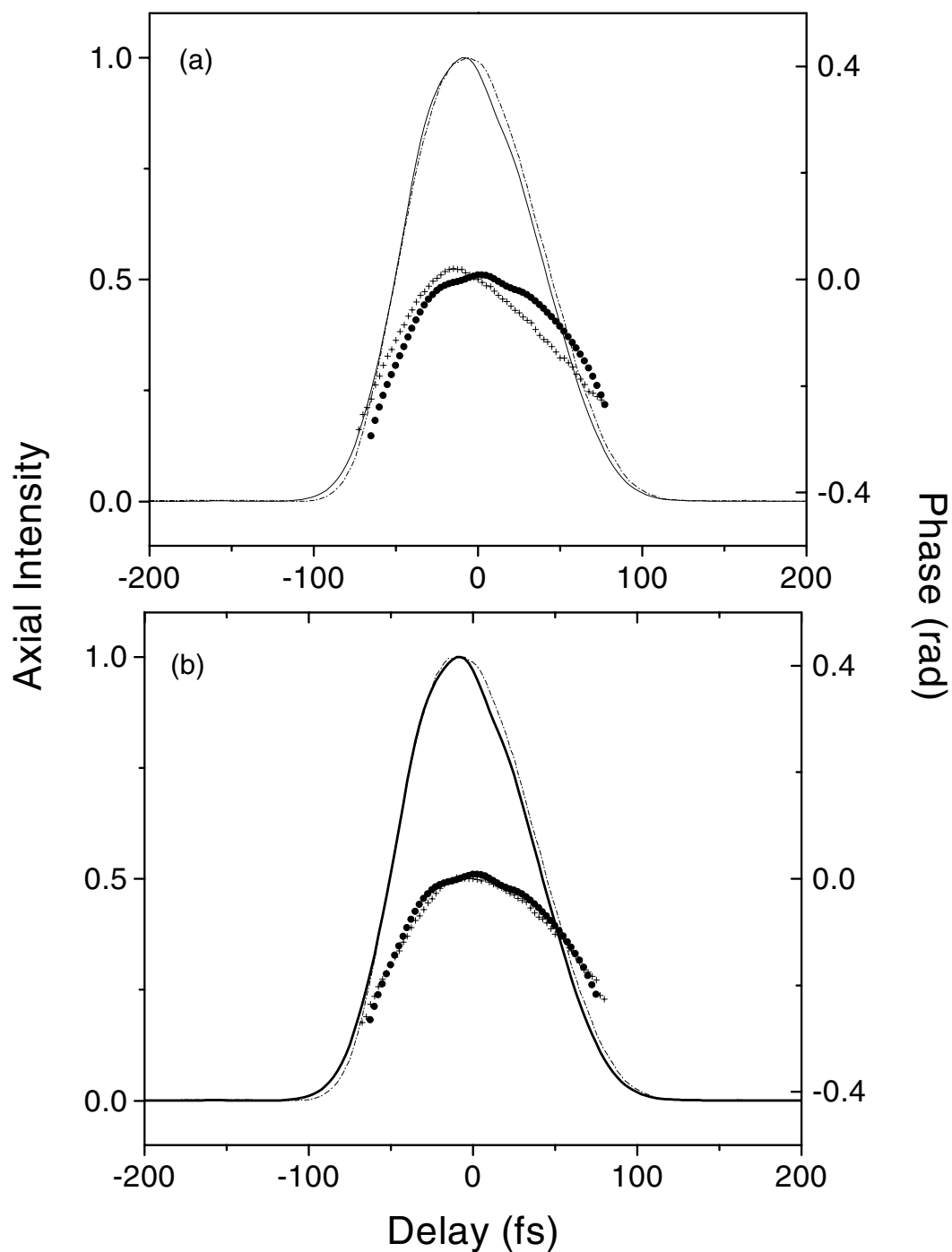


Figure 6.2: Calculated field after propagation (a) assuming an instantaneous nonlinearity and (b) with inclusion of a non-instantaneous nonlinearity. The calculated intensity is plotted as a dashed line and the calculated phase is plotted as crosses. The calculated fields are shown along with the measured field (solid line and points) for comparison.

whether the observed response is indeed a result of the nonlinear index of refraction changing during the measurement, we also performed measurements using a flowing methanol apparatus.

6.1.2 Flowing Methanol Measurements

Experiment

For these experiments, a dye cell and pump from a dye laser were used to flow the sample. A new dye cell was used to ensure that there was no contamination from an optically active dye. The path length through the sample was 1.69 cm, and the thickness of the cell walls was 2 mm. In addition, a vacuum spatial filter was inserted into the beam path before the sample cell to improve the spatial quality of the beam. Peak input powers ranged between 4.5 and 5.5 GW. Again, all experiments were performed in the plane wave regime. It is also important to note that all of the data in the remainder of this chapter were acquired under sub-optimal laboratory conditions. The building temperature fluctuated over a range of seven degrees Celsius from day to night, greatly affecting laser performance and stability. As a result, all FROG traces were acquired in duplicate and only data from those traces that were repeatable are presented here. Careful observation of the beam with PG FROG was also used to monitor changes in laser behavior. In this way, if the laser changed between the measurement of two repeatable reference traces and two repeatable sample traces, the data were also discarded.

Data

Figure 6.3 shows the intensity and phase of the input field and the field after propagation through 1.69 cm of methanol. The input pulse has an intensity FWHM of 120 fs and has a nearly flat phase with a small component of upchirp. After propagation, the pulse is broadened in time and is significantly upchirped as is evidenced by the

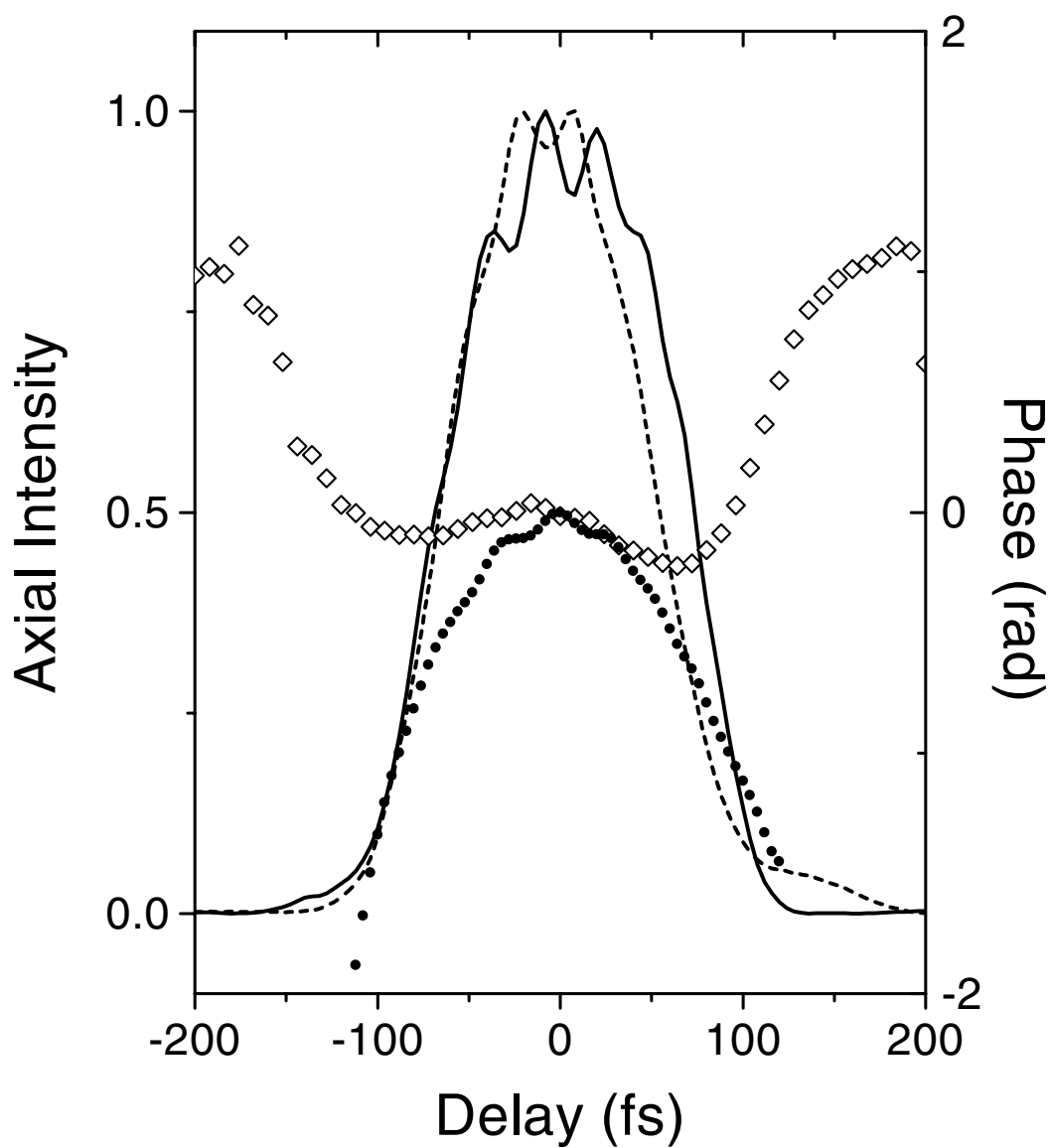


Figure 6.3: Measured intensity and phase of the pulse before (dashed line and diamonds) and after (solid line and points) traversing 1.69 cm of methanol.

downward curvature of the phase. These features are a result of the interplay between SPM with positive n_2 and positive dispersion. A shift in the phase toward the trailing edge of the pulse is difficult to discern by eye.

The corresponding spectra before and after propagation through the methanol sample are shown in Fig. 6.4. After propagation through the methanol, a red-shift of energy in the spectrum is observed. This spectral red-shifting is indicative of a non-instantaneous nonlinearity.

Propagation with a very upchirped input pulse was also investigated. For this data, the input power was increased such that the peak intensity was roughly the same as for the shorter, flat-phase pulse. This experiment thus tests for any dependence of the non-instantaneous nonlinearity on the chirp or length of the pulse. The temporal duration of the very chirped input pulse differs from that of the nearly flat-phase input pulse by 12 fs. The phase of the very chirped input pulse changes by approximately six radians from the center of the pulse to the point where the intensity has dropped to $1/e^2$ of the peak intensity. The most obvious effect of the propagation is a significant broadening of the pulse. Thirty-five femtoseconds more pulse broadening is observed with this upchirped input than with the nearly flat-phase input of Fig 6.3. This extra broadening is the result of an upchirped input pulse providing a head start to the propagation-induced upchirp that results from SPM with positive n_2 and positive GVD.

Model and Results

The flowing methanol data are modeled using the same equations as the stationary cell data. The cell walls in this case are approximately twice as thick (2 mm) as the walls of the stationary cell. Including propagation through the cell walls in the calculation has an observable effect on the calculated spectra. Therefore, all calculations are performed assuming propagation first through 2 mm of fused silica with values of

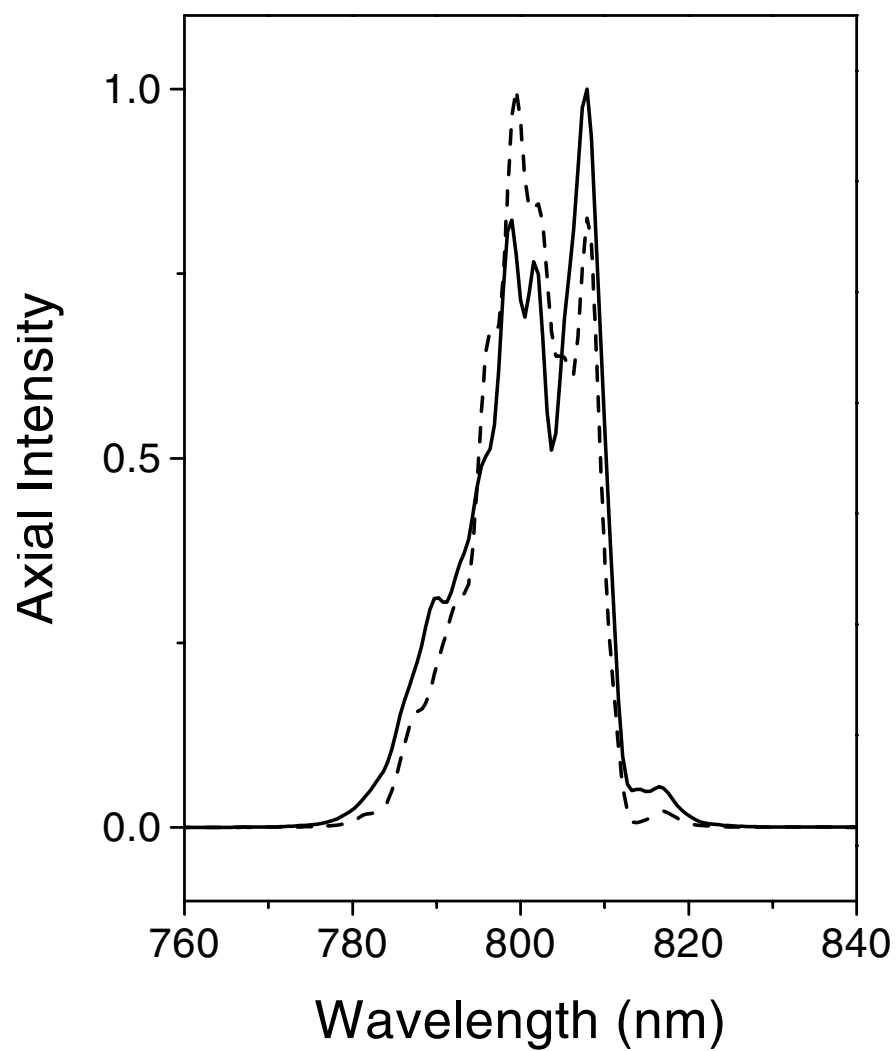


Figure 6.4: Measured spectra before (dashed line) and after (solid line) propagation through 1.69 cm of methanol.

$n_2 = 2.5 \times 10^{-16} \text{ cm}^2/\text{W}$ and $k'' = 360 \text{ fs}^2/\text{cm}$ and assuming an instantaneous response. The field is then propagated numerically through the methanol sample using $k'' = 290 \text{ fs}^2/\text{cm}$, assuming a non-instantaneous nonlinearity as given by Eq. 6.3 and varying the values of n_2 and τ . Finally, the field is propagated through the second 2 mm wall of fused silica.

Calculations using the measured input field from Fig. 6.3 are in best agreement with the temporal broadening of the measured field after propagation when a value of $n_2 = 4 \times 10^{-16} \text{ cm}^2/\text{W}$ is used. Figure 6.5 shows the measured intensity and phase along with calculated results using this value of n_2 and three different values of τ . If the nonlinearity is assumed to be purely instantaneous ($\tau = 0$), the calculated phase does not match well on the leading or trailing edges of the pulse. On the other hand, when τ is assumed to be 27 fs (the value determined by Nibbering *et al.*), the calculated phase is shifted too far toward the trailing edge of the pulse. The best match between the model and experiment is found when a value of $\tau = 10$ fs is used. To further illustrate this point, the differences between the measured and calculated phases for these three values of τ are plotted in Fig. 6.6. The phase difference in the case of $\tau = 10$ fs always falls between the phase differences in the other two cases, and is on average closer to zero. The small scale modulation in the measured phase is not reproduced by the calculations and results in the modulations seen in all three of the phase difference curves. Performing calculations on a much finer grid might reproduce these modulations. Currently, the largest number of points in the field array that the model can handle is 512.

A comparison between the measured spectrum after propagation (shown in Fig. 6.4) and the calculated spectrum corresponding to the case of $\tau = 10$ fs (Fig. 6.5) is shown in Fig. 6.7. The measured and calculated spectra are in good agreement. The calculation reproduces the observed shifting of energy to the red spectral components.

Calculations involving the very upchirped input pulse also show good agreement

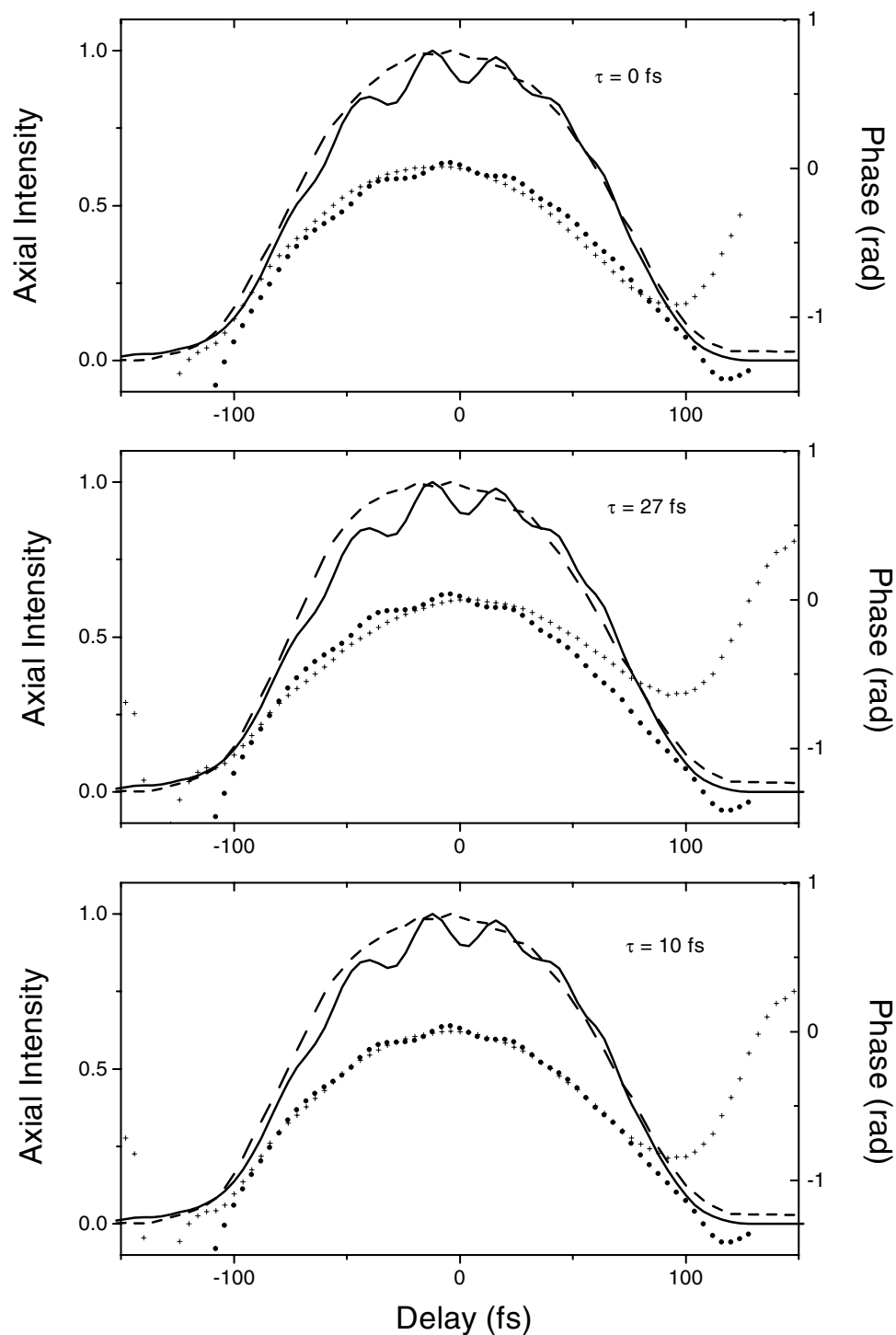


Figure 6.5: Measured intensity (solid line) and phase (points) along with calculated intensity (dashed line) and phase (crosses) using the input field from Fig. 6.3 with $n_2 = 4 \times 10^{-16} \text{ cm}^2/\text{W}$ for three different values of τ .

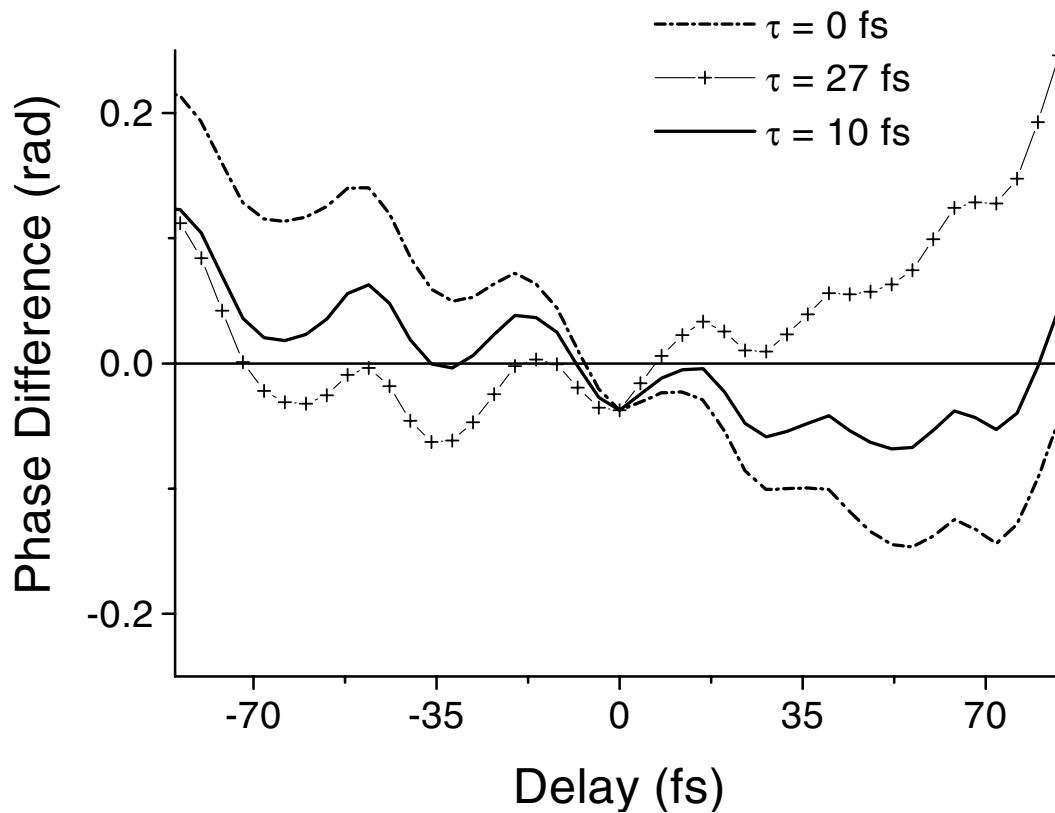


Figure 6.6: The difference between measured and calculated phase for the three calculations presented in Fig. 6.5: $\tau = 0$ fs (dots and dashes), $\tau = 10$ fs (solid line) and $\tau = 27$ fs (line with crosses).

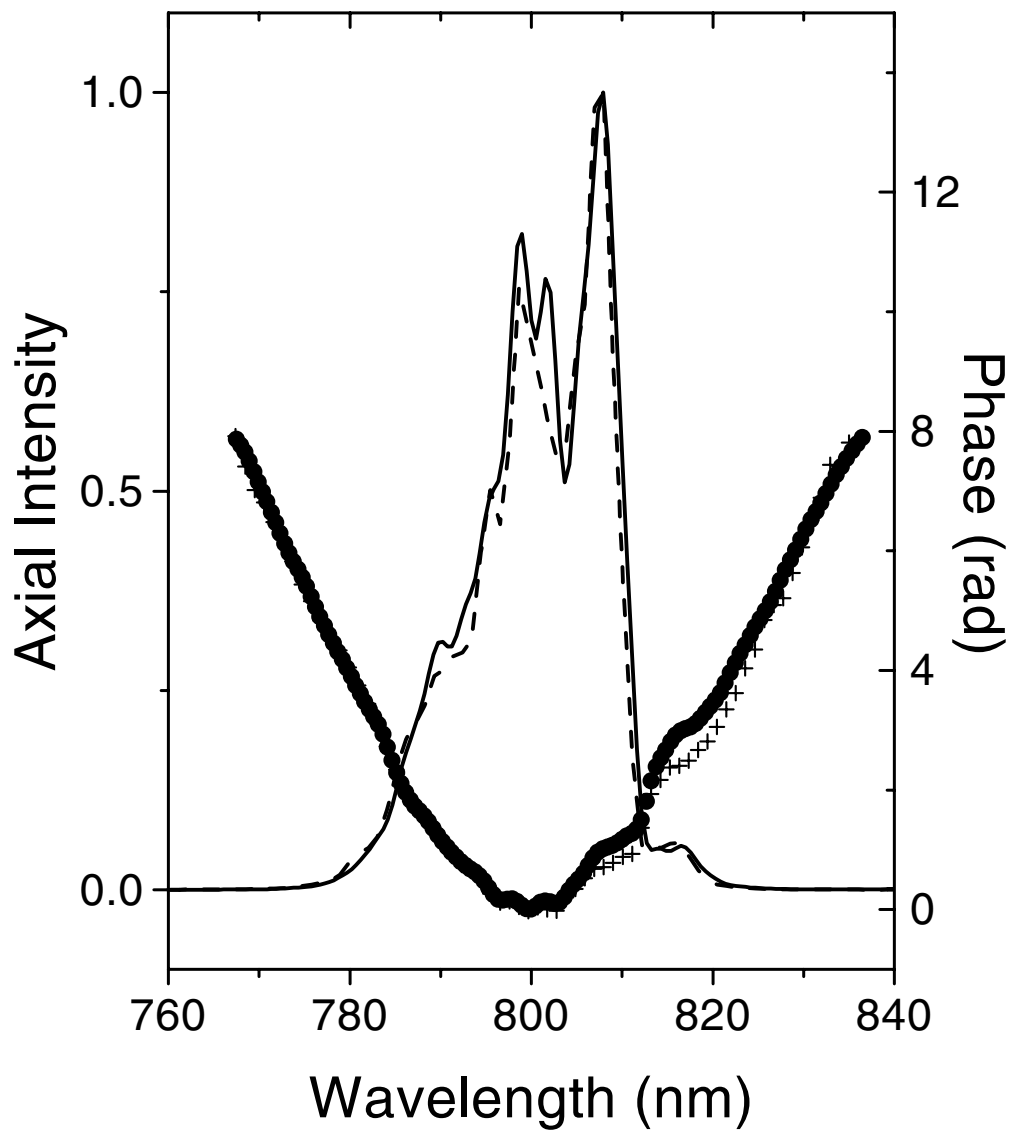


Figure 6.7: Measured spectral intensity and phase (solid line and points) along with calculated spectral intensity and phase (dashed line and crosses) for the case of $n_2 = 4 \times 10^{-16} \text{ cm}^2/\text{W}$ and $\tau = 10 \text{ fs}$.

with experiment when values of $n_2 = 4 \times 10^{-16} \text{ cm}^2/\text{W}$ and $\tau = 10 \text{ fs}$ are used in the model. The phase in this case is so strongly curved, however, that the effects of differing values of τ are difficult to distinguish. Therefore, any dependence of the non-instantaneous nonlinearity on the chirp of the pulse is difficult to extract. Moreover, it is best to use a flat-phase input pulse in experiments to determine the value n_2 and τ .

6.1.3 Discussion

The data presented in the previous two sections clearly indicate the presence of a non-instantaneous nonlinearity in methanol. Experiments with a flowing methanol configuration rule out the possibility that heating effects are contributing to the measured nonlinearity. In all cases, we observe values of n_2 and τ that are smaller than those reported by Nibbering *et al.* [94]. To demonstrate that our numbers are clearly different from those measured by Nibbering, a plot of our data with a calculation using Nibbering's numbers is shown in Fig. 6.8. The calculated field is very different from the measured field in this case.

There are several questions that should be addressed. The first is the difference in the measured values reported in these two investigations. The model used to calculate the nonlinear response is the same in both cases. The two main differences in the approaches are the experimental method used and the length of the input pulses. Nibbering's work involves propagating 150 fs pulses through the sample. Since these pulses are longer, it is possible that they measure contributions to the nonlinear index from libration and rotation (response time of 100 fs) that the shorter pulses used in our experiment do not detect. It is also possible that there is a systematic error in one or both of the measurement techniques that results in the differing magnitudes of the propagation parameters. Another possible difference lies in the method of measuring the input intensity. A small change in the input intensity results in a noticeable change in the magnitude of the nonlinear index of refraction. Therefore an incorrectly cali-

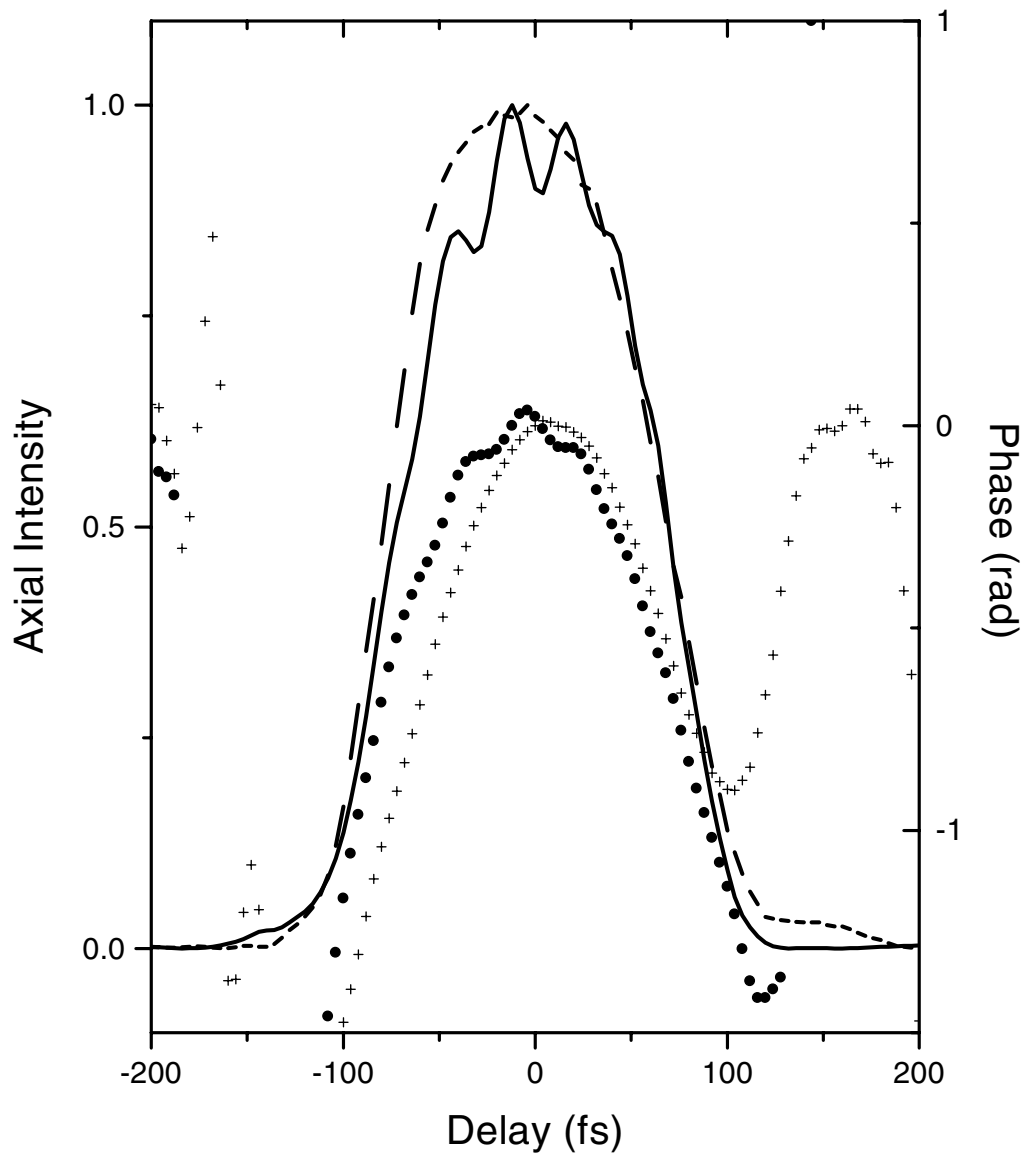


Figure 6.8: Measured intensity and phase (solid line and points) with calculated intensity and phase (dashed line and crosses) using Nibbering's reported values: $n_2 = 6.7 \times 10^{-16} \text{ cm}^2/\text{W}$ and $\tau = 27 \text{ fs}$.

brated power meter, or an inaccurate assessment of input pulse duration, could lead to the differences in the measured values of n_2 .

A second question that remains is the nature of the non-instantaneous nonlinearity. Most effects involving nuclear or molecular motion respond on timescales much longer than 10 fs. If this effect is real, one may ask whether it is possible that the cause is not actually something that occurs with a 10 fs response time, but simply results in a phase profile that has similar characteristics. The model is one used to describe any diffusive retardation in the medium and is not necessarily representative of the true nature of the process or processes involved. The presence of one- or two-photon absorptions affecting the nonlinear index is ruled out by the UV-Vis absorption spectrum of methanol which is flat between 850 nm and 205 nm. In addition, two-photon absorption is typically accompanied by a flattening of the peak of the intensity profile after propagation [158], a feature that is not observed in our data. Also, measurements of power throughput reveal losses due only to reflection.

A third question surrounding the observed effect is whether it could be an artifact of the measurement techniques used. To partially respond to this question, we perform experiments in water using the same techniques. Water is chosen because like methanol, it is a small, polar liquid that is hydrogen bonded and has a flat UV-Vis absorption spectrum down to 190 nm.

6.2 Water Studies

Water measurements are performed using the flowing liquid apparatus described in Section 6.1.2. Peak input powers are always near 5 GW, and the pulses propagate as plane waves through the sample. The stability criteria are again used to select which data sets to analyze. Calculations are performed taking into account propagation through the cell walls. Fisher HPLC-grade water is used as the sample.

This work		Previous work		
n_2 (10^{-16} cm ² /W)	# data sets	n_2 (10^{-16} cm ² /W)	wavelength	Ref.
1.8	2	2.8	694 nm	[159]
3.0	1	4.2	532 nm	[160]
4.5	3	5.4	532 nm	[159]
		5.7	804 nm	[94]

Table 6.1: Measured and literature values of n_2 for water.

6.2.1 Data and Results

Figure 6.9 shows the measured intensity and phase before and after propagation through 1.69 cm of water. The input pulse has an initial upchirp that leads to enhanced broadening of the pulse. After propagation, the pulse is more upchirped and shows no shifting of the phase toward the trailing edge of the pulse.

Calculations are performed using the measured input field and a value of $k'' = 247$ fs²/cm [156]. For all acquired data, the best fit is obtained when only an instantaneous nonlinearity is included. A comparison of the calculated and measured fields after propagation for the data shown in Fig. 6.9 is plotted in Fig. 6.10. The calculated intensity and phase matches the measurement quite well. For this calculation, $n_2 = 1.8 \times 10^{-16}$ cm²/W. The fact that no non-instantaneous nonlinearity is present in water indicates that the nonlinearity observed for methanol is not likely an artifact of the measurement technique.

The value of n_2 was determined for several data sets by using n_2 as a fit parameter in calculating the measured field. Three different values were obtained, with an average value of 3.4 ± 0.4 cm²/W accounting for random error only. In all cases the agreement between the measured and calculated fields were comparable to that shown in Fig. 6.10. Table 6.1 shows our measured values along with some values from the literature. Beside each measured value is the number of data sets that gave that result. Our measured values are somewhat lower than the only other published value near 800 nm [94]. The

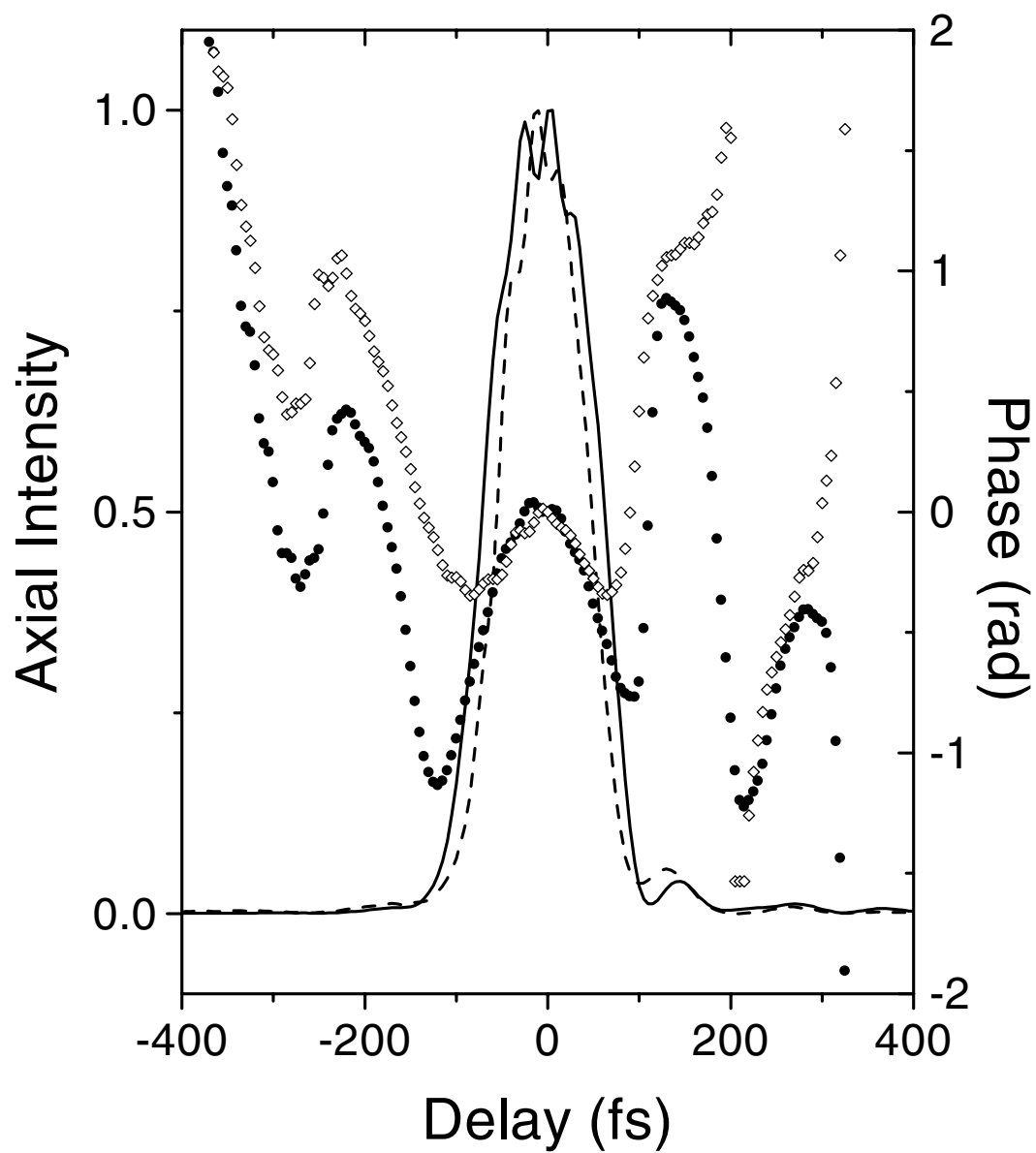


Figure 6.9: Measured intensity and phase prior to (dashed line and diamonds) and after (solid line and points) propagation through 1.69 cm of water.

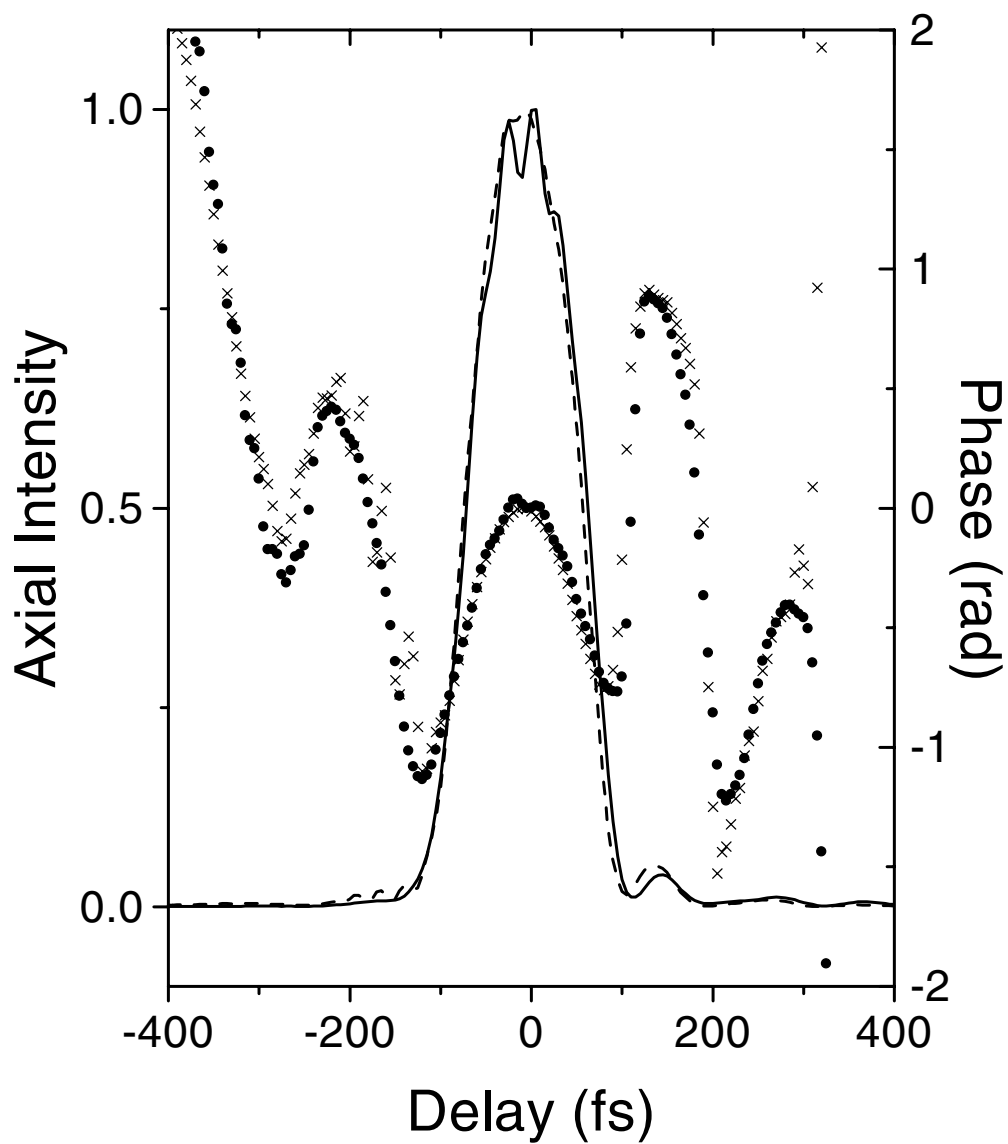


Figure 6.10: Measured (solid line and points) and calculated (dashed line and crosses) intensity and phase after propagation through 1.69 cm of water. The calculation assumes a purely instantaneous nonlinearity.

spread in the values of n_2 given by different data sets is larger than we would ideally like it to be. There are several possible explanations for this. One problem may involve accurate measurement of the intensity. Measurement of the peak intensity is based on accurate knowledge of the area of the input pulse (see Chapter 3). If the area of the input pulse changes between measurement of the input pulse and measurement of the pulse after propagation through the sample, the intensity, and hence n_2 , will be incorrect. With the unstable room conditions present during these measurements, it is conceivable that small scale or very slow changes could have occurred without causing the data to fail the stability requirements. Also, during these water measurements a problem arose with the temperature servo on the baseplate of the regenerative amplifier. The temperature of the baseplate fluctuated over several degrees Celsius during the course of an hour. Fluctuations in the temperature of the amplifier baseplate affect laser performance and could contribute to the observed inconsistencies in the data. One could also argue that the observed differences are an inherent limit of the measurement technique. Previous FROG data presented in this thesis gives much more repeatable results, however. It is more likely a problem of accurate measurement of the intensity of an unstable laser.

6.3 Summary

The experiments in this chapter corroborate the existence of a non-instantaneous nonlinearity with a very short response time in methanol. The value of this response time is found to be 10 fs, roughly three times shorter than the previous measurement reported [94]. Experiments conducted with a flowing methanol apparatus eliminate the possibility that the observed nonlinearity is actually a heating effect. The shorter pulses used in these experiments also cast doubt on the mechanism being driven by librational motion. Experiments in water, which show a purely instantaneous nonlinearity, confirm that the measured non-instantaneous nonlinearity in methanol is probably real.

Measurements of power throughput, observations of the temporal intensity of the pulse after propagation, and observations of the UV-Vis absorption spectrum of methanol all indicate that there is no evidence for absorption occurring during propagation. The actual mechanism responsible for the observed non-instantaneous nonlinearity remains undetermined.

Attempts to measure the nonlinear index of refraction of water using this technique gave results with low precision. The results, however, are in agreement with other values published in the literature. And, under more stable conditions, this would likely be a reasonable method of measuring the nonlinear index of refraction.